International Journal of Innovative Computing, Information and Control
Volume **22**, Number **2**, April **2026**

ICIC International ©2026 ISSN 1349-4198
pp. **413–429**

CONTROL SYSTEM USING MULTI-PERIOD DISTURBANCE OBSERVER FOR MINIMUM-PHASE SYSTEMS

Siripong Sangsarpan[1,2], Daisuke Koyama[2], Nghia Thi Mai[3]
Md Abdus Samad Kamal[2], Iwanori Murakami[2] and Kou Yamada[2,*]

[1]Faculty of Engineering
Thai-Nichi Institute of Technology
1771/1 Suanluang, Bangkok 10250, Thailand
siripong@tni.ac.th

[2]Graduate School of Science and Technology
Gunma University
1-5-1 Tenjincho, Kiryu 376-8515, Japan
{ t232b002; maskamal; murakami }@gunma-u.ac.jp; *Corresponding author: yamada@gunma-u.ac.jp

[3]Faculty of Electronics Engineering 1
Posts and Telecommunications Institute of Technology
122 Hoang Quoc Viet Road, Cau Giay District, Hanoi 122300, Vietnam
nghiamt@ptit.edu.vn

Received August 2025; revised December 2025

Abstract. *This paper considers a control system design for minimum-phase systems that ensures the output follows the non-periodic reference input and periodic disturbances are attenuated without repetitive control. In practical applications, a control system often has to attenuate periodic disturbances and make the output follow a non-periodic reference input. To achieve these requirements, repetitive control has been proposed. Repetitive control can attenuate periodic disturbances. However, repetitive control typically results in high-order controllers. To design a low-order controller that attenuates periodic disturbances, the control system has to be designed without using repetitive control. In this paper, the control system using a multi-period disturbance observer to attenuate periodic disturbances is proposed. The multi-period disturbance observer uses a low-order filter, and attenuate periodic disturbances using the period of disturbances. Since the multi-period disturbance observer uses a low-order filter, it becomes possible to design the low-order controller. However, there are no studies about a design method of the control system using the multi-period disturbance observer. To design a low-order controller attenuating periodic disturbances, the transfer function from the disturbance to the output must have a finite number of poles. A condition that the transfer function from the disturbance to the output has a finite number of poles is clarified. In addition, the internal stability condition of the control system using the multi-period disturbance observer that makes the number of poles finite is clarified. Based on these above conditions, a design method of the control system using the multi-period disturbance observer is also proposed.*

Keywords: Disturbance observer, Disturbance attenuation, Low sensitivity control, Minimum-phase systems, Multi-period disturbance observer

1. **Introduction.** Disturbance attenuation remains a critical issue in precision control systems. According to the internal model principle, effective attenuation of step and ramp disturbances requires the controller to include integrators or poles that match these disturbances. However, many practical systems are perturbed by periodic disturbances

DOI: 10.24507/ijicic.22.02.413

composed of multiple harmonics, which can significantly degrade accuracy, particularly in precision motion and power-conversion applications.

These challenges motivate low-order designs that address multi-harmonic periodic disturbances without resorting to high-order internal models. To effectively attenuate periodic disturbances, repetitive control that embeds an internal model has been proposed [1]. In repetitive control, the controller places poles on the imaginary axis that coincide with the harmonics of the periodic input. By the internal-model principle, embedding an infinite set of such poles yields strong attenuation at the harmonic frequencies. Repetitive control is suitable for tracking periodic reference input with high accuracy and for periodic-disturbance attenuation. For non-periodic references, Pipeleers et al. developed a repetitive-control design [2].

However, repetitive control has some limitations. A limitation of repetitive control is the undesired magnitude amplification at non-repetitive frequencies [3]. From the Bode integral theorem, repetitive control typically worsens the amplitude of the response at frequencies other than the one where performance is improved. Moreover, embedding the internal model typically leads to high-order compensators, which increase computational and tuning burden. These limitations motivate low-order alternatives that can address multi-harmonic periodic disturbances without resorting to infinite internal models. Recent extensions of repetitive-control ideas confirm the sustained interest in harmonic rejection but also highlight persistent issues of controller order and tuning burden; hence, a low-order alternative that avoids embedding infinite internal models is desirable [4, 5, 6].

For tracking non-periodic reference input, repetitive control is not always necessary to make the output follow non-periodic references. To attenuate disturbances, a disturbance observer is often used [7]. A disturbance observer estimates disturbances from available measurements. Since the estimated disturbance by the disturbance observer can be used to attenuate disturbances, many papers propose control systems using a disturbance observer [8, 9, 10]. Kim et al. proposed a general-form disturbance observer that can estimate high-order disturbances in the time domain [8]. Na et al. proposed a continuous-time repetitive-control design aided by a disturbance observer for time-delay systems with periodic references and disturbances [9]. Comprehensive reviews of disturbance observer research are available in [10]. Because of its structural simplicity, the disturbance observer has seen wide applications [7, 11, 12, 13, 14, 15, 16, 17]. The disturbance observer is used for an application in a factory plant [13, 18]. In a motion control field, the disturbance observer is often used to cancel the disturbances or to make the closed-loop system robustly stable [7, 14, 15, 16, 17].

From a robust-control viewpoint, Mita et al. pointed out that disturbance observers are not the only alternative for complete controller design [19]. In [19], extended H_∞ control was proposed as an effective motion-control method for disturbance cancellation. From another viewpoint, Kobayashi et al. considered an observer design method for obtaining phase compensation based on disturbance observers [20]. Compared with phase-compensator-based designs, the control system in [20] is simple and easy to design. In this way, robustness analyses of control systems incorporating disturbance observed have been considered.

Another important control problem of the disturbance observer is the parameterization problem, which is the problem of finding all disturbance observers for plants [21]. If the parameterization of all disturbance observers is obtained, we can express previous research of disturbance observers in a uniform manner. In addition, disturbance observers could be designed systematically. From this viewpoint, parameterizations of all disturbance observers and all linear functional disturbance observers for plants with any input-output disturbances are examined [21, 22, 23, 24, 25]. Yamada et al. clarified the parameterization

of all disturbance observers for disturbances with finitely many frequency components [21]. For periodic disturbances, a periodic disturbance observer was proposed [22, 23, 24]. In [22, 23, 24], the parameterization of all periodic disturbance observers for periodic output disturbance, periodic input disturbance and periodic input-and-output disturbance is presented. The periodic disturbance observer does not always make the control system stable. Yamada et al. considered this problem and proposed a control system using the periodic disturbance observer for the periodic output disturbance [26]. The results of [22, 23, 24, 26] have a remaining problem in that their method uses only one signal of the periodic time before the present time. Phukapak et al. proposed a multi-period disturbance observer and clarified the parameterization of all multi-period disturbance observers for periodic output disturbances [25]. The multi-period disturbance observer can use multiple signals of the periodic time before the present time.

However, no paper has examined a concrete design method for a control system using a multi-period disturbance observer to attenuate periodic disturbances. This paper proposes a design method for a control system that uses a multi-period disturbance observer to attenuate periodic disturbances without using repetitive control. In contrast to repetitive control, the proposed framework maintains a low controller order and admits a closed-form synthesis that ensures a finite-pole disturbance-to-output transfer function.

This paper is organized as follows. Section 2 explains the problem considered in this paper and proposes the control system using a multi-period disturbance observer for periodic disturbance. Section 3 clarifies a condition that the transfer function from the disturbance to the output has a finite number of poles. Section 4 clarifies a stability condition of the proposed control system. Section 5 shows the control characteristics of the proposed control system. Section 6 considers a design of controllers for disturbance attenuation. Section 7 provides a design method of the control system to attenuate the multi-periodic disturbances effectively and to follow the non-periodic reference input without steady-state error using the disturbance observer. In Section 8, the numerical example is illustrated to show the effectiveness of the proposed design method. Section 9 gives concluding remarks.

2. Problem Formulation.

Consider the plant described by

$$\begin{cases} \dot{x}(t) = Ax(t) + Bu(t) \\ y(t) = Cx(t) + d(t) \end{cases}, \tag{1}$$

where $x(t) \in R^n$ is the state variable, $u(t) \in R$ is the control input, $y(t) \in R$ is the output, $d(t) \in R$ is the periodic disturbance with period $T > 0$ satisfying

$$d(t+T) = d(t) \quad (\forall t > 0), \tag{2}$$

$A \in R^{n\times n}$, $B \in R^n$ and $C \in R^{1\times n}$. It is assumed that (A, B) is stabilizable, (C, A) is detectable, A has no eigenvalue on the imaginary axis, that is,

$$\det \begin{bmatrix} A - sI & B \\ C & 0 \end{bmatrix} = 0 \tag{3}$$

has no root in the closed right half plane, and $u(t)$ and $y(t)$ are available, but $d(t)$ is unavailable.

From (1), we have

$$y(s) = G(s)u(s) + d(s), \tag{4}$$

where

$$G(s) = C(sI - A)^{-1}B \in R(s). \tag{5}$$

Here, $y(s)$, $u(s)$ and $d(s)$ are denoted as $y(s) = \mathcal{L}[y(t)]$, $u(s) = \mathcal{L}[u(t)]$ and $d(s) = \mathcal{L}[d(t)]$, respectively. Note that the assumption in (3) implies that $G(s)$ has no zero in the closed right half plane, that is, $G(s)$ is of minimum-phase.

To design a control system such that the output $y(t)$ follows the non-periodic reference input $r(t)$ and the periodic disturbance $d(t)$ is attenuated, we adopt the multi-period disturbance observer for the output periodic disturbance in [25]. Using the multi-period disturbance observer for periodic disturbances in [25], we propose a control system shown in Figure 1. Here, $C_1(s) \in R(s)$ is the feedback controller, and $C_2(s)$ is the controller for multi-period disturbance observer. $r(s) \in R(s)$ is the non-periodic reference input $r(s) = \mathcal{L}[r(t)] \in R(s)$, $d_1(s) \in R(s)$ and $d_2(s) \in R(s)$ are input signals to the control system in Figure 1. Since the available measurements of the plant in (1) are $u(s)$ and $y(s)$, $d(s)$ is estimated by the form in

$$\tilde{d}(s) = \sum_{k=1}^{N} F_{1k}(s)e^{-sT_k}y(s) + \sum_{k=1}^{N} F_{2k}(s)e^{-sT_k}u(s), \tag{6}$$

where $F_{1k}(s) \in RH_\infty$ $(k = 1, \ldots, N)$ is of minimum-phase, $F_{2k}(s) \in RH_\infty$ $(k = 1, \ldots, N)$ is of minimum-phase, and $T_k \in R > 0$ is defined by

$$T_k = kT \ (k = 1, 2, \ldots, N). \tag{7}$$

According to [25], $\tilde{d}(s)$ in (6) is called the multi-period disturbance observer if

$$e_d(s) = d(s) - \tilde{d}(s) \tag{8}$$

satisfies

$$\lim_{t\to\infty} e_d(t) = \lim_{t\to\infty} \left(d(t) - \tilde{d}(t)\right) = 0, \tag{9}$$

where $e_d(t) = \mathcal{L}^{-1}[e_d(s)]$.

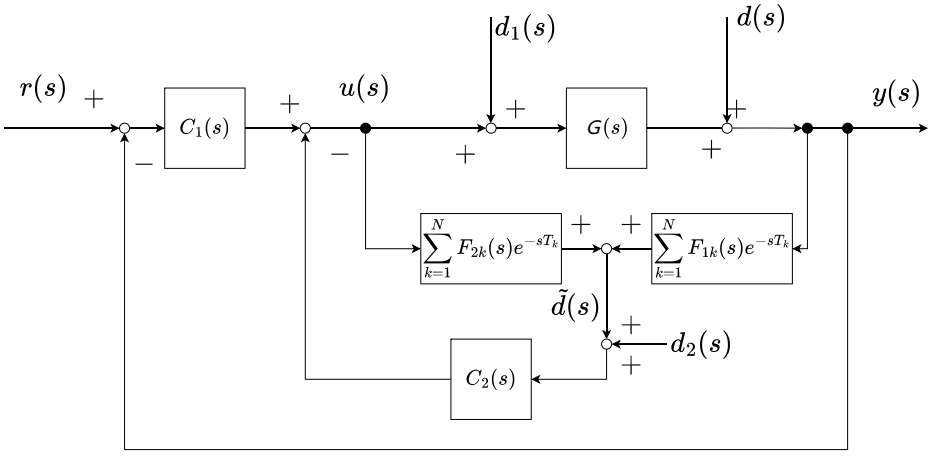

FIGURE 1. The control system using the multi-period disturbance observer

The parameterization of all $F_{1k}(s) \in RH_\infty$ $(k = 1, \ldots, N)$ and $F_{2k}(s) \in RH_\infty$ $(k = 1, \ldots, N)$ satisfying (9) for any initial state $x(0)$, the control input $u(t)$ and the periodic output disturbance $d(t)$ is given by

$$\sum_{k=1}^{N} F_{1k}(s) = D(s) + Q(s)D(s) \tag{10}$$

and

$$\sum_{k=1}^{N} F_{2k}(s) = -N(s) - Q(s)N(s), \tag{11}$$

where $D(s)$ and $N(s)$ are coprime factors of $G(s)$ on RH_∞ satisfying

$$G(s) = \frac{N(s)}{D(s)} \tag{12}$$

and $Q(s) \in RH_\infty$ is any function satisfying

$$D(s_k) + Q(s_k)D(s_k) = 1 \quad \forall s_k \ (k = 0, 1, \ldots), \tag{13}$$

$$s_k = j\omega_k, \tag{14}$$

$$\omega_k = \frac{2\pi k}{T} \tag{15}$$

and j is the imaginary unit [25].

Using the multi-period disturbance observer for periodic disturbances, in general, the transfer function from the disturbance $d(s)$ to the output $y(s)$ has an infinite number of poles. In order to make the transfer function from $d(s)$ to $y(s)$ have a finite number of poles, $C_2(s)$ is chosen in the form

$$C_2(s) = \frac{C_n(s)}{1 + \sum_{k=1}^{N} C_{dk}(s)e^{-sT_k}}, \tag{16}$$

where $C_n(s) \in R(s)$ and $C_{dk}(s) \in R(s)$ $(k = 1, \ldots, N)$.

The problem in this paper is to propose a design method for the control system in Figure 1 to attenuate the periodic disturbance $d(s)$, for the output $y(s)$ to follow the reference input $r(s)$ and to make the transfer function from $d(s)$ to $y(s)$ have a finite number of poles.

3. Condition for a Finite Number of Poles.

In this section, we clarify the condition that the transfer function from $d(s)$ to $y(s)$ in Figure 1 has a finite number of poles.

From Figure 1, the transfer function from $d(s)$ to $y(s)$ is given by

$$\frac{y(s)}{d(s)} = \frac{1 + \sum_{k=1}^{N} \left\{ \left(C_{dk}(s) + C_n(s)F_{2k}(s) \right) e^{-sT_k} \right\}}{1 + G(s)C_1(s) + \sum_{k=1}^{N} \left\{ \left(1 + G(s)C_1(s) \right) C_{dk}(s) + C_n(s)\left(F_{2k}(s) + G(s)F_{1k}(s) \right) \right\} e^{-sT_k}}. \tag{17}$$

From this equation, we have the following theorem.

Theorem 3.1. *The transfer function from $d(s)$ to $y(s)$ in (17) has a finite number of poles if and only if the following expression holds true.*

$$\left(1 + G(s)C_1(s) \right) C_{dk}(s) + \left\{ C_n(s)F_{2k}(s) + C_n(s)G(s)F_{1k}(s) \right\} = 0 \ (k = 1, \ldots, N). \tag{18}$$

Proof: Necessity is shown. That is, we show that if the transfer function from $d(s)$ to $y(s)$ has a finite number of poles, then (18) is satisfied. From the assumption that the transfer function from $d(s)$ to $y(s)$ has a finite number of poles,

$$\sum_{k=1}^{N} \left\{ \left(1 + G(s)C_1(s) \right) C_{dk}(s) + C_n(s) \left(F_{2k}(s) + G(s)F_{1k}(s) \right) \right\} e^{-sT_k} = 0 \tag{19}$$

is satisfied. This is equivalent to (18). Thus, the necessity is shown.

Next, the sufficiency is shown. That is, if the equation of (18) holds true, then the transfer function of the control system shown in Figure 1 has a finite number of poles. From the assumption that the equation of (18) holds true, we have

$$\sum_{k=1}^{N} \left\{ \left(1 + G(s)C_1(s)\right) C_{dk}(s) + C_n(s) \left(F_{2k}(s) + G(s)F_{1k}(s)\right) \right\} e^{-sT_k} = 0. \tag{20}$$

Thus, the transfer function of the control system shown in Figure 1 has a finite number of poles. □

4. **Stability Condition.** In this section, we clarify the stability condition for the control system in Figure 1. From the definition of internal stability [27], in order to keep the stability of the control system in Figure 1, all signals in the closed loop have to be bounded for every set of bounded inputs $r(s)$, $d(s)$, $d_1(s)$ and $d_2(s)$ in Figure 1.

From this, we have the following theorem.

Theorem 4.1. *Assume that the transfer function from $d(s)$ to $y(s)$ in (17) has a finite number of poles. The control system in Figure 1 is internally stable if and only if the following expressions hold true.*

1) $C_1(s)$ stabilizes $G(s)$.
2) $C_{dk}(s) \in RH_\infty$ $(k = 1, 2, \ldots, N)$ in (16).
3) $C_n(s) \in RH_\infty$ in (16).

Proof: From the assumption that the transfer function from $d(s)$ to $y(s)$ in (17) has a finite number of poles, (18) holds true. From the definition of internal stability, the control system shown in Figure 1 is internally stable if and only if all functions $V_{ij}(s)$ $(i = 1, 2, 3;$ $j = 1, 2, 3, 4)$ belong to RH_∞, where $V_{ij}(s)$ is a function denoted as

$$\begin{bmatrix} y(s) \\ u(s) \\ \tilde{d}(s) \end{bmatrix} = \begin{bmatrix} V_{11}(s) & V_{12}(s) & V_{13}(s) & V_{14}(s) \\ V_{21}(s) & V_{22}(s) & V_{23}(s) & V_{24}(s) \\ V_{31}(s) & V_{32}(s) & V_{33}(s) & V_{34}(s) \end{bmatrix} \begin{bmatrix} r(s) \\ d(s) \\ d_1(s) \\ d_2(s) \end{bmatrix} \tag{21}$$

with inputs $d_1(s) \in R(s)$ and $d_2(s) \in R(s)$ in Figure 1. Here all functions $V_{ij}(s)$ $(i = 1, 2, 3;$ $j = 1, 2, 3, 4)$ are described as

$$V_{11}(s) = \frac{\left(1 + \sum_{k=1}^{N} C_{dk}(s)e^{-sT_k}\right) G(s)C_1(s)}{1 + C_1(s)G(s)}, \tag{22}$$

$$V_{12}(s) = \frac{\left(1 + \sum_{k=1}^{N} C_{dk}(s)e^{-sT_k}\right) + C_n(s) \sum_{k=1}^{N} F_{1k}(s)e^{-sT_k}}{1 + C_1(s)G(s)}, \tag{23}$$

$$V_{13}(s) = \frac{G(s)C_n(s)}{1 + C_1(s)G(s)}, \tag{24}$$

$$V_{14}(s) = \frac{G(s)\left(1 + \sum_{k=1}^{N} C_{dk}(s)e^{-sT_k}\right)}{1 + C_1(s)G(s)}, \tag{25}$$

$$V_{21}(s) = \frac{C_1(s)\left(1 + \sum_{k=1}^{N} C_{dk}(s)e^{-sT_k}\right)}{1 + C_1(s)G(s)}, \tag{26}$$

$$V_{22}(s) = \frac{C_1(s)\left(1 + \sum_{k=1}^{N} C_{dk}(s)e^{-sT_k}\right) + C_n(s) \sum_{k=1}^{N} F_{2k}(s)e^{-sT_k}}{1 + C_1(s)G(s)}, \tag{27}$$

$$V_{23}(s) = \frac{C_n(s)}{1 + C_1(s)G(s)}, \tag{28}$$

$$V_{24}(s) = \frac{1 + \sum_{k=1}^{N} C_{dk}(s)e^{-sT_k}}{1 + C_1(s)G(s)}, \tag{29}$$

$$V_{31}(s) = \frac{\left(1+\sum_{k=1}^{N} C_{dk}(s)e^{-sT_k}\right)C_1(s)G(s)\sum_{k=1}^{N}F_{1k}(s)e^{-sT_k}+C_n(s)\sum_{k=1}^{N}F_{2k}(s)e^{-sT_k}}{1 + G(s)C_1(s)}, \tag{30}$$

$$V_{32}(s) = \frac{\left(1 + \sum_{k=1}^{N} C_{dk}(s)e^{-sT_k}\right)\left(\sum_{k=1}^{N} F_{1k}(s)e^{-sT_k} + C_1(s)\sum_{k=1}^{N} F_{2k}(s)e^{-sT_k}\right)}{1 + G(s)C_1(s)}, \tag{31}$$

$$V_{33}(s) = \frac{C_n(s)\left(G(s)\sum_{k=1}^{N} F_{1k}(s)e^{-sT_k} + \sum_{k=1}^{N} F_{2k}(s)e^{-sT_k}\right)}{1 + G(s)C_1(s)} \tag{32}$$

and

$$V_{34}(s) = \frac{\left(1 + \sum_{k=1}^{N} C_{dk}(s)e^{-sT_k}\right)\left(G(s)\sum_{k=1}^{N} F_{1k}(s)e^{-sT_k} + \sum_{k=1}^{N} F_{2k}(s)e^{-sT_k}\right)}{1 + G(s)C_1(s)}. \tag{33}$$

The remaining problem is to show that $V_{ij}(s) \in RH_\infty$ $(i = 1, 2, 3;\ j = 1, 2, 3, 4)$ is equivalent to the expressions 1, 2, and 3. The necessity is shown. That is, we show that if the control system in Figure 1 is stable, then $C_1(s)$ stabilizes $G(s)$, $C_n(s) \in RH_\infty$ and $C_{dk}(s)$ $(k = 1, \ldots, N) \in RH_\infty$. From (22)-(33), the control system shown in Figure 1 is stable, then zeros of $1 + G(s)C_1(s)$ must be in the open left half plane. According to [27], this is equivalent to expression 1. Since $C_1(s)$ stabilizes $G(s)$ and $V_{ij}(s) \in RH_\infty$, it is clear that $C_n(s) \in RH_\infty$ and $\sum_{k=1}^{N} C_{dk}(s) \in RH_\infty$. This is equivalent to expressions 2 and 3. From the above discussion, we prove the necessity of Theorem 4.1.

The sufficiency is shown. That is, if $C_1(s)$ stabilizes $G(s)$, $C_{dk}(s) \in RH_\infty$ $(k = 1, 2, \ldots, N)$, $C_n(s) \in RH_\infty$ in (16), then the control system in Figure 1 is internally stable. From the assumption that $C_1(s)$ stabilizes $G(s)$, $C_{dk}(s) \in RH_\infty$ $(k = 1, 2, \ldots, N)$ and $C_n(s) \in RH_\infty$ in (16), it is clear that all functions $V_{ij}(s) \in RH_\infty$ $(i = 1, 2, 3;\ j = 1, 2, 3, 4)$ in (21).

From the above discussion, we have proved Theorem 4.1. □

5. **Control Characteristics.** In this section, we consider the control characteristics of the control systems in Figure 1.

An input-output property of the control system in Figure 1 is specified by the transfer function from $r(s)$ to $y(s)$ written by

$$y(s) = \frac{G(s)C_1(s)}{1 + G(s)C_1(s)}r(s). \tag{34}$$

From (34), (10) and (11), the error $e(s) = r(s) - y(s)$ can be written as

$$e(s) = \frac{1}{1 + C_1(s)G(s)}\, r(s). \tag{35}$$

From the internal model principle [28], for the output $y(s)$ to follow the non-periodic reference input $r(s)$ without steady state error, $C_1(s)$ needs to be written in the form

$$C_1(s) = C_r(s)\bar{C}_1(s), \tag{36}$$

where $C_r(s)$ is the internal model of $r(s)$ and $\bar{C}_1(s) \in R(s)$ has no zero of unstable poles of $C_r(s)$.

The disturbance attenuation characteristics of the control system in Figure 1 are specified by the transfer function from periodic disturbance $d(s)$ to the output $y(s)$ written by

$$y(s) = \frac{1 + \sum_{k=1}^{N} \left\{ \left(C_{dk}(s) + C_n(s) F_{2k}(s) \right) e^{-sT_k} \right\}}{1 + G(s) C_1(s)} d(s). \tag{37}$$

From (37) and simple manipulation, if

$$\sum_{k=1}^{N} \left\{ \delta_k + \left(C_{dk}(s) + C_n(s) F_{2k}(s) \right) \right\} \Big|_{s=s_k} = 0 \ (k = 1, 2, \ldots,), \tag{38}$$

then the periodic disturbance $d(s)$ is attenuated, where δ_k $(k = 1, \ldots, N)$ is arbitrary real number satisfying $\sum_{k=1}^{N} \delta_k = 1$. From (38), we have

$$\delta_k + \left(C_{dk}(s) + C_n(s) F_{2k}(s) \right) \big|_{s=s_k} = 0. \tag{39}$$

From (39), the disturbance attenuation characteristics are specified using $C_d(s)$ and $C_n(s)$ of $C_2(s)$ in (16).

Thus, the purpose of $C_1(s)$ is to satisfy the input-output property, and the purpose of $C_2(s)$ is to satisfy the disturbance attenuation characteristics. This implies that the control system shown in Figure 1 is a two-degree-of-freedom control system.

6. **Design of Controllers $C_1(s)$ and $C_2(s)$.** In this section, we consider a design of controllers $C_1(s)$ and $C_2(s)$ for disturbance attenuation. In order to have a finite number of poles and to make a multi-periodic disturbance attenuate, (18) and (39) should be satisfied.

From the discussion in the previous sections, $C_n(s)$ and $C_{dk}(s)$ of $C_2(s)$ in (16) and $C_1(s)$ need to satisfy (18) and (39). From (39), if $C_n(s)$ and $C_d(s)$ satisfy

$$\sum_{k=1}^{N} C_{dk}(s) + C_n(s) \sum_{k=1}^{N} F_{2k}(s) = -1, \tag{40}$$

then $C_n(s)$ and $C_{dk}(s)$ satisfy (39). Substituting (40) into (18), we obtain $C_n(s)$. However, $C_n(s)$ obtained by (18) and (40) is not always proper.

To overcome this problem, we change the problem to satisfy (39) by

$$\sum_{k=1}^{N} C_{dk}(s) + C_n(s) \sum_{k=1}^{N} F_{2k}(s) = -q(s), \tag{41}$$

where $q(s) \in RH_\infty$ is a strictly proper low-pass filter given by

$$q(s) = \frac{1}{(1 + \tau s)^n}, \tag{42}$$

$n > 0$ is an arbitrary positive integer chosen so that $C_n(s)$ becomes proper and $\tau > 0$ is an arbitrary small real number. The low-pass filter $q(s)$ in (42) can attenuate the periodic disturbance $d(s)$ with frequency component ω_l satisfying

$$q(j\omega_l) \simeq 1 \ \left(\omega_l = \frac{2\pi l}{T}; l = 0, 1, \ldots, l_{\max} \right), \tag{43}$$

where $l_{\max}$ is a maximum integer to be attenuated. From (41) and (11), $C_n(s)$ can be rewritten by

$$C_n(s) = -\frac{q(s) + \sum_{k=1}^{N} C_{dk}(s)}{\sum_{k=1}^{N} F_{2k}(s)} = \frac{q(s) + \sum_{k=1}^{N} C_{dk}(s)}{\left(1 + Q(s)\right) N(s)}. \tag{44}$$

From Theorem 3.1, $C_n(s)$ and $C_{dk}(s)$ should satisfy (18). From (18), (10), and (11), simple manipulation gives

$$
\begin{aligned}
&(1+G(s)C_1(s))\sum_{k=1}^{N} C_{dk}(s) + C_n(s)\left(\sum_{k=1}^{N} F_{2k}(s) + G(s)\sum_{k=1}^{N} F_{1k}(s)\right) \\
&= (1+G(s)C_1(s))\sum_{k=1}^{N} C_{dk}(s) \\
&= 0. \qquad (45)
\end{aligned}
$$

Since it is obvious that $1 + G(s)C_1(s) \neq 0$, we have

$$\sum_{k=1}^{N} C_{dk}(s) = 0. \qquad (46)$$

Substitution of (46) to (44) yields

$$C_n(s) = \frac{q(s)}{(1+Q(s))\,N(s)}. \qquad (47)$$

From the above discussion, $C_n(s)$ and $C_{dk}(s)$ $(k = 1, \ldots, N)$ are designed to satisfy (46) and (47).

7. **Design Method of the Control System.** In this section, we provide a design procedure of the control system shown in Figure 1. Using the above expressions, a design procedure of the control system in Figure 1 is summarized as follows:

Design Procedure

Step 1. Obtain a pair of coprime factors $N(s)$ and $D(s)$ of $G(s)$ in (12).
Step 2. Find the period T of disturbance $d(t)$.
Step 3. Set N in (6). T_k $(k = 1, \ldots, N)$ is given by (7).
Step 4. $Q(s) \in RH_\infty$ is designed satisfying (13) and making $1 + Q(s)$ of minimum-phase. Then, $F_{1k}(s)$ $(k = 1, \ldots, N)$ and $F_{2k}(s)$ $(k = 1, \ldots, N)$ are designed satisfying (10) and (11), respectively.
Step 5. Spacify the reference input $r(t)$. Obtain the internal model $C_r(s)$ corresponding to $r(t)$.
Step 6. $C_1(s)$ is designed to satisfy (36) and to stabilize $G(s)$.
Step 7. $q(s) \in RH_\infty$ in (41) is settled as (42) according to the frequency components of the disturbance $d(t)$.
Step 8. $C_2(s)$ in (16) is designed. $C_{dk}(s) \in RH_\infty$ $(k = 1, \ldots, N)$ is settled to satisfy (46). $C_n(s)$ is given by (47).

8. **Numerical Example.** In this section, a numerical example is presented to demonstrate the effectiveness of the proposed design method.

Consider the problem of designing the control system in Figure 1 to attenuate the multi-periodic disturbance $d(s)$ with period $T = 2\pi$ and for the output $y(s)$ to follow the ramp reference input $r(s) = 1/s^2$, and to make the transfer function from $d(s)$ to $y(s)$ have a finite number of poles for the minimum-phase system $G(s)$ written by

$$G(s) = \frac{s+1}{s^2 - 43s - 350}. \qquad (48)$$

Coprime factors $N(s)$ and $D(s)$ of $G(s)$ in (48) satisfying (12) are given by

$$N(s) = \frac{s+1}{s^2 + 2s + 1}, \qquad (49)$$

and

$$D(s) = \frac{s^2 - 43s - 350}{s^2 + 2s + 1}. \tag{50}$$

To attenuate the multi-periodic disturbance $d(s)$ with $T = 2\pi$, $F_{1k}(s)$ and $F_{2k}(s)$ are designed as

$$F_{1k}(s) = \frac{1}{N} \frac{-(1.074\,s^2 + 1.892\,s + 0.993)\,(s-50)(s+7)}{(s+1)^2\,(s^2 + 57s + 350)} \tag{51}$$

and

$$F_{2k}(s) = \frac{1}{N} \frac{1.074\,s^2 + 1.892\,s + 0.993}{(s+1)\,(s^2 + 57s + 350)} \tag{52}$$

where N is any integer, $k = 1, 2, \ldots, N$, and $Q(s)$ in (10) and (11) satisfying (13) is settled as

$$Q(s) = -\frac{2.074s^2 + 58.892s + 350.993}{s^2 + 57s + 350}. \tag{53}$$

From a simple calculation, $Q(s)$ in (53) satisfies (13). Moreover, $1 + Q(s)$ is minimum phase.

$C_1(s)$ is designed to satisfy (36) and to stabilize $G(s)$. We use

$$C_1(s) = \frac{200(s+1)(s+100)}{s^2}. \tag{54}$$

$C_1(s)$ in (54) has two poles at the origin. This implies that $1/s^2$ in (54) acts as the internal model for ramp reference input $r(t)$.

We choose the low-pass filter

$$q(s) = \frac{1}{1 + 0.001s}. \tag{55}$$

From (16), (47) and (46), $C_2(s)$ is designed as

$$C_2(s) = -\frac{(s^2 + 57s + 350)(s^2 + 2s + 1)}{(0.001s + 1)(1.074s^2 + 1.892s + 0.993)(s+1)}. \tag{56}$$

The effectiveness of the control system in Figure 1 about the disturbance attenuation is considered. Figure 2 shows the response of the output $y(t)$ in Figure 1 when $N = 3$, for the disturbance $d(t)$ given by

$$d(t) = \sum_{i=1}^{3} \sin(it). \tag{57}$$

The dotted line in Figure 2 shows $d(t)$ in (57), and the solid line in Figure 2 shows the response of the output $y(t)$ from the control system in Figure 1 when $N = 3$ for the disturbance $d(t)$ in (57). From Figure 2, it is clear that the control system in Figure 1 when $N = 3$ makes the response of $y(t)$ for $d(t)$ in (57) be close to 0. Figure 3 shows the response of the error $e(t) = r(t) - y(t)$ on the control system in Figure 1 when $N = 3$ for a ramp reference input $r(t) = t$. From Figure 3, the error $e(t)$ is close to 0 after 20 [sec]. This implies that the control system in Figure 1 when $N = 3$ has the performances of tracking the non-periodic reference input.

The performances of the control system in Figure 1 when $N = 3$ are compared with those of the following four control methods.

(i) **OL** – Feedforward control,
(ii) **DF** – Feedback control only using unity gain,
(iii) **DF** + C_1 – The feedback control only using $C_1(s)$ without disturbance observers,
(iv) **DOB** – The control system in Figure 1 when $N = 1$.

Here, the control system in Figure 1 when $N = 1$ is the same as the control system using the periodic disturbance observer in [26]. The performance of the above four control methods (i), (ii), (iii), (iv) and the proposed control system in Figure 1 when $N = 3$ is evaluated by comparing the response of $y(t)$ for $d(t)$ in (57) from 0 [sec] to 30 [sec]. To compare the performance of the above four control methods (i), (ii), (iii), (iv) and the proposed control system in Figure 1, the following four indicators are used.

- Integral of squared error (ISE) given by

$$\int_0^{30} y(t)^2 dt, \tag{58}$$

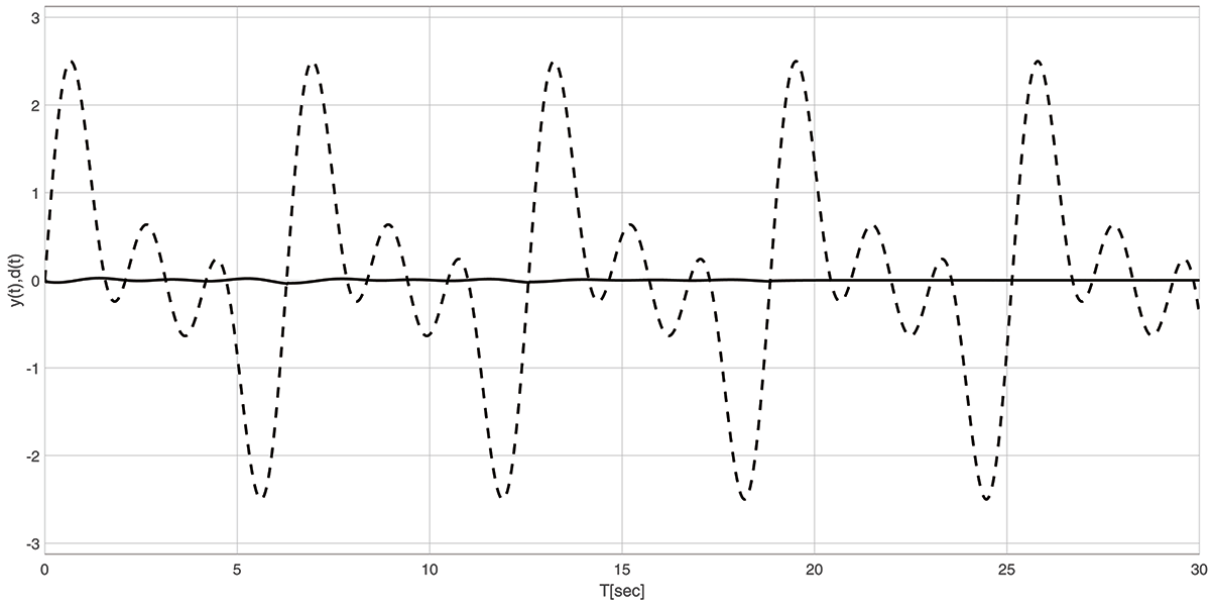

FIGURE 2. Response of the output $y(t)$ for the disturbance $d(t)$ in (57)

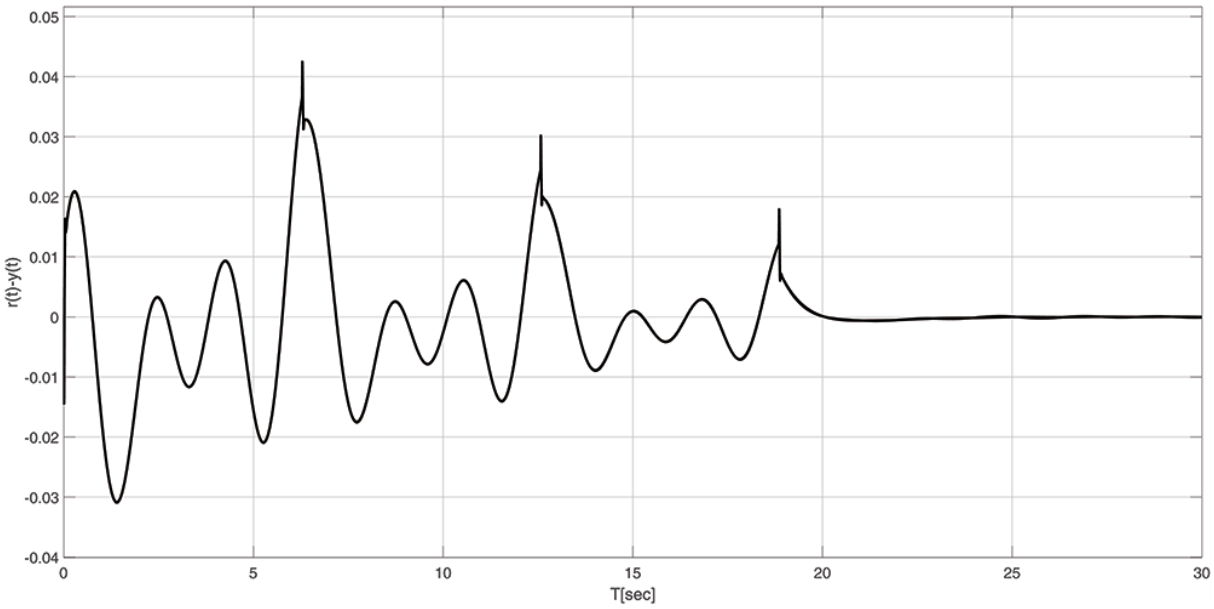

FIGURE 3. Response of the error $e(t) = r(t) - y(t)$ for the ramp reference input $r(t) = t$

- Integral of absolute error (IAE) given by

$$\int_0^{30} |y(t)|dt, \tag{59}$$

- Root-mean-square error (RMS) given by

$$\sqrt{\frac{1}{30}\int_0^{30} y(t)^2 dt}, \tag{60}$$

- The percentage improvement based on the RMS.

The RMS directly reflects the average magnitude of the error over a period from 0 [sec] to 30 [sec]. A lower RMS indicates that the corresponding control systems attenuate the disturbance more effectively. The percentage improvement based on the RMS is an indicater denoted by

$$\text{Improvement}_{\text{RMS}}(\%) = \frac{\text{RMS}_{\text{other}} - \text{RMS}_{\text{Proposed}}}{\text{RMS}_{\text{other}}} \times 100. \tag{61}$$

The percentage improvement in (61) represents the difference between the RMS of each of the four control methods and that of the proposed control system in Figure 1 when $N = 3$. The results of the performances of the control system in Figure 1 and the methods (i), (ii), (iii) and (iv) are shown in Table 1. Here, the column of **Proposed** in Table 1 shows the result of the control system in Figure 1 when $N = 3$. From Table 1, the RMS of the proposed control system in Figure 1 when $N = 3$ is lower than those of control methods (i), (iii) and (iv) except for method (ii), which makes the response of $y(t)$ for $d(t)$ in (57) diverge. The RMS of the control system in Figure 1 when $N = 1$ achieves 0.07408, but its performance rapidly degrades under period mismatch and multi-frequency disturbances.

Table 1. Steady-state tracking error metrics

Strategy	ISE	IAE	RMS	Improvement [%]
OL	42.6383	26.0273	1.19215	91.68
DF	∞	∞	∞	100
DF + C_1	0.92368	4.12084	0.17547	43.48
DOB	0.16447	0.94963	0.07408	−33.87
Proposed	**0.29495**	**1.81477**	**0.09917**	**—**

To show the effectiveness of the proposed design method of the control system in Figure 1, we compare the control system in Figure 1 when $N = 3$ and that of $N = 1$.

To confirm the performance of tracking $r(t) = t$, the error $e(t) = r(t) - y(t)$ for $r(t) = t$ of the control system in Figure 1 when $N = 3$ and that of the control system in Figure 1 when $N = 1$ are shown in Figure 4. Here, the solid line in Figure 4 shows the error $e(t)$ of the proposed control system in Figure 1 when $N = 3$ and the dotted line in Figure 4 shows the error $e(t)$ of the control system in Figure 1 when $N = 1$. In Figure 4, the error $e(t)$ for $r(t) = t$ of the proposed control system using the multi-period disturbance observer in Figure 1 when $N = 3$ is the same as that of the control system in Figure 1 when $N = 1$.

The response of the output $y(t)$ for $d(t)$ in (57) from the control system using the multi-periodic disturbance observer in Figure 1 when $N = 3$ and that of $N = 3$ is also shown in Figure 5. Here, the solid line shows the response of $y(t)$ for $d(t)$ in (57) from the proposed control system in Figure 1 when $N = 3$, and the dotted line shows the response

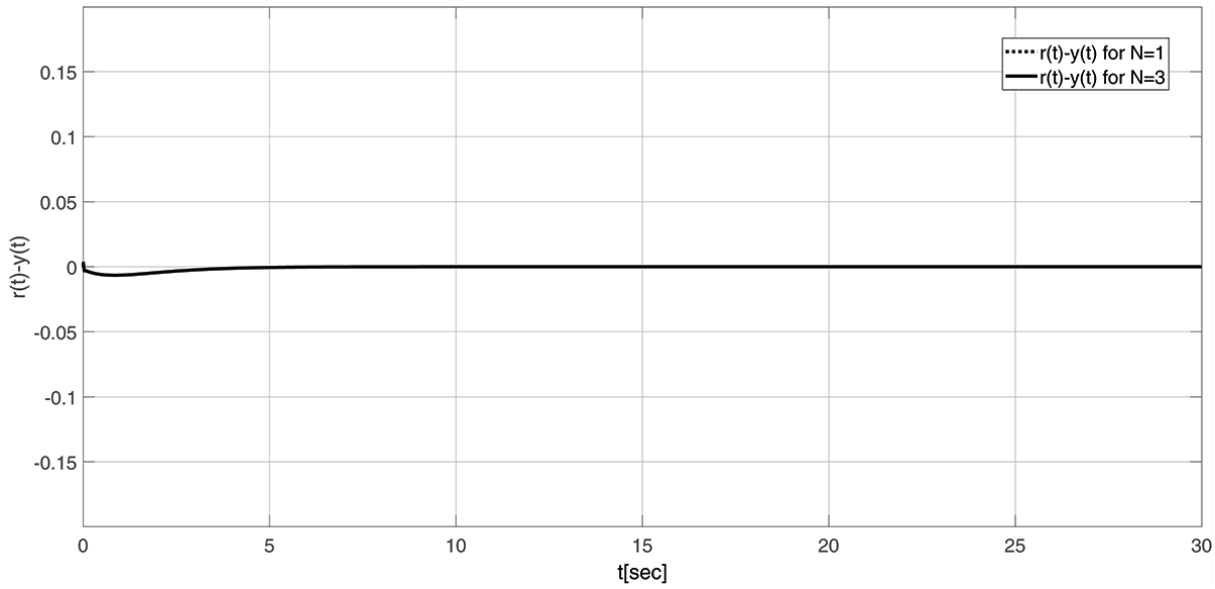

FIGURE 4. The response of error $e(t) = r(t) - y(t)$ when $N = 1$ and $N = 3$

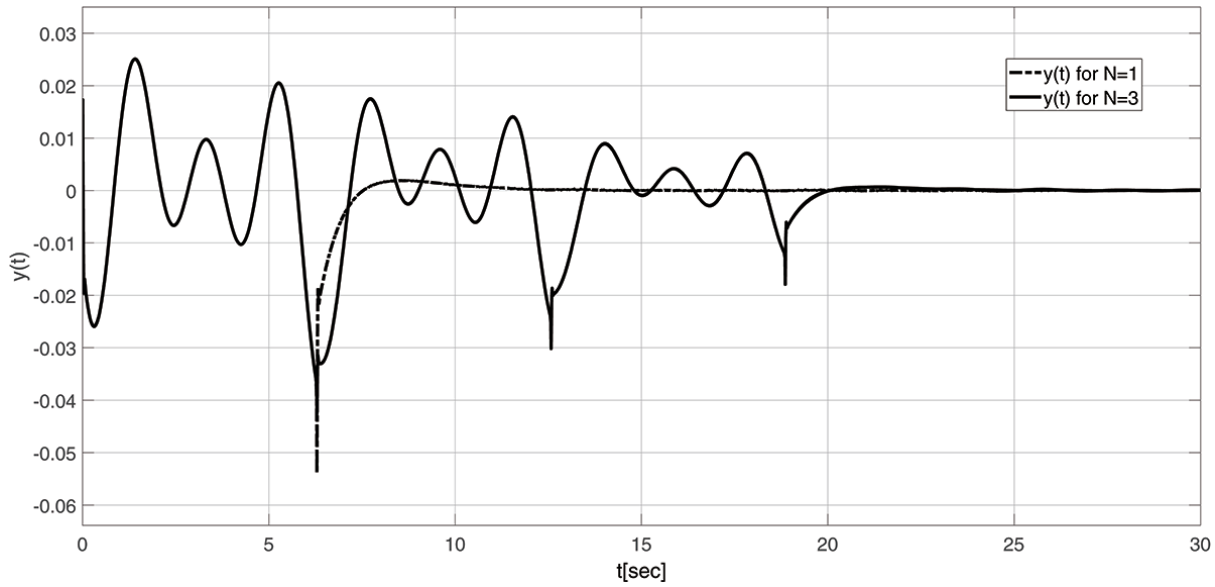

FIGURE 5. The response of the output $y(t)$ for the disturbance $d(t)$ in (57)

of $y(t)$ for $d(t)$ in (57) from the control system in Figure 1 when $N = 1$. In Figure 5, the maximum absolute value of $y(t)$ for $d(t)$ in (57) in the proposed control system using the multi-periodic disturbance observer in Figure 1 when $N = 3$ is smaller than that of the control system in Figure 1 when $N = 1$.

The control characteristics of the control system in Figure 1 when the actual period of disturbance $d(t)$ differs from $T = 2\pi$ are confirmed. The response of $y(t)$ for $d(t)$ with $T = 4\pi$ from the proposed control system in Figure 1 when $N = 3$ and that of $N = 1$ are shown in Figure 6. In Figure 6, the solid line shows the response of $y(t)$ for $d(t)$ with $T = 4\pi$ from the proposed control system in Figure 1 when $N = 3$, and the dotted line shows the response of $y(t)$ for $d(t)$ with $T = 4\pi$ from the control system in Figure 1 when $N = 1$. From Figure 6, it causes the ripple in the response of $y(t)$ for $d(t)$ with $T = 4\pi$ from the control system in Figure 1 when $N = 3$ and that of $N = 1$. In the case of $N = 3$, the

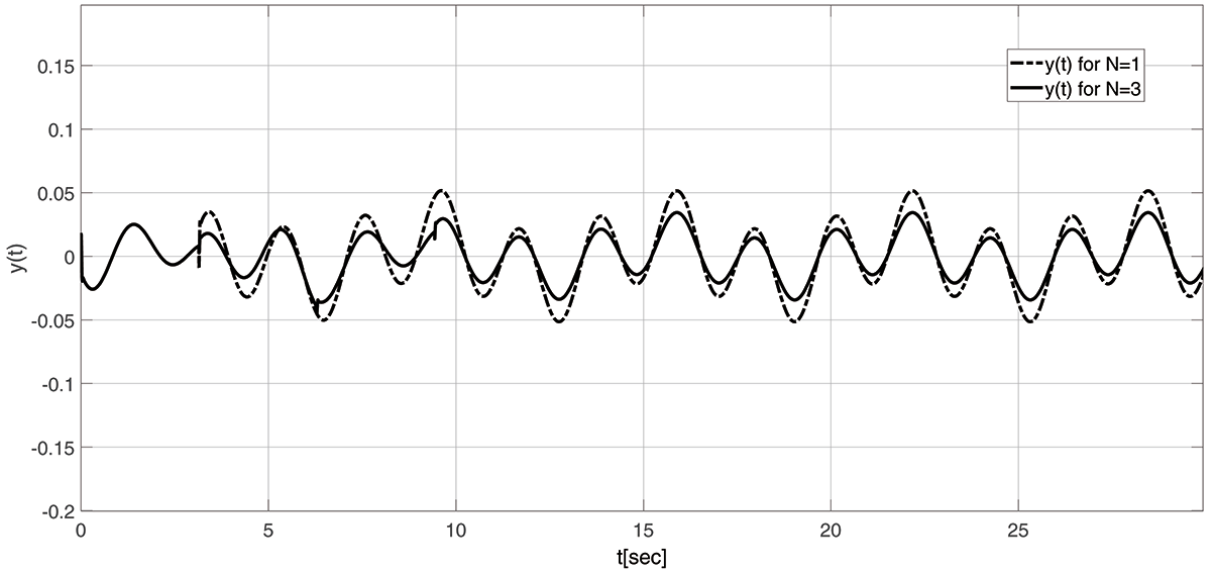

FIGURE 6. The response of the output $y(t)$ for the disturbance with the period 4π

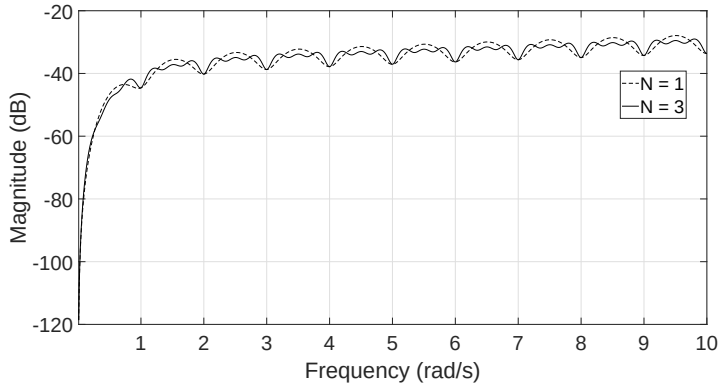

FIGURE 7. Gain plots of the transfer function from $d(s)$ to $y(s)$ for the control system in Figure 1 when $N = 3$ and that of $N = 1$

absolute value of the ripple of $y(t)$ for $d(t)$ in Figure 1 in the steady-state is approximately $|y(t)|_{\max} \approx 2.950 \times 10^{-2}$. In the case of $N = 1$, the absolute value of the ripple of $y(t)$ for $d(t)$ in Figure 1 in the steady-state is approximately $|y(t)|_{\max} \approx 5.156 \times 10^{-2}$. Thus, the ripple in the response of $y(t)$ for $d(t)$ from the proposed control system in Figure 1 when $N = 3$ is smaller than that of $N = 1$. This implies that the proposed control system in Figure 1 when $N = 3$ attenuates periodic disturbances more effectively than the control system in Figure 1 when $N = 1$.

The gain plot of the transfer function from $d(s)$ to $y(s)$ for the control system in Figure 1 when $N = 3$ and that of $N = 1$ is shown in Figure 7. From Figure 7, at every 1 dB intervals, the maximum gain of the transfer function from $d(s)$ to $y(s)$ for the control system in Figure 1 when $N = 3$ is smaller than that of $N = 1$. This implies that the proposed control system in Figure 1 when $N = 3$ can attenuate the disturbances, which has the difference period from $T = 2\pi$, more than that of $N = 1$.

9. **Conclusion.** This paper proposed a design method for the control system using the multi-periodic disturbance observer for the single-input/single-output minimum-phase

systems. Using the proposed control system, we have designed a control system to attenuate the periodic disturbance without using repetitive control. The condition that the transfer function from the disturbance to the output has a finite number of poles is clarified. The internal stability condition of the control system using the multi-periodic disturbance observer is also clarified. The control system using the multi-periodic disturbance observer can make the ripple in the response of the output for the periodic disturbance be smaller than that of using the periodic disturbance observer, even if the period of actual periodic disturbances differs from that of the period considered when the control system is designed. The control system using the multi-period disturbance observer can be applied to the design of control systems with disturbance attenuation for periodic disturbances. However, this paper does not consider an application of the proposed control system. In addition, this control system cannot be applied to time-varying disturbances. These will be considered in another paper.

REFERENCES

[1] M. Nakano, T. Inoue, Y. Yamamoto and S. Hara, Repetitive control, *The Society of Instrument and Control Engineers*, 1989 (in Japanese).

[2] G. Pipeleers, B. Demeulenaere, J. D. Schutter and J. Swevers, Robust high-order repetitive control: Optimal performance trade-offs, *Automatica*, vol.44, no.10, pp.2628-2634, 2008.

[3] K. Nie, W. Xue, C. Zhang and Y. Mao, Disturbance observer-based repetitive control with application to optoelectronic precision positioning system, *Journal of the Franklin Institute*, vol.358, no.16, pp.8443-8469, 2021.

[4] E. Kurniawan, H. Wang, J. A. Prakosa, P. Purwowibowo and E. B. Pratiwi, An improved repetitive controller with fractional time-delay for discrete-time linear systems: Synthesis and comparison study, *ISA Transactions*, vol.146, pp.511-527, 2024.

[5] J. Reinders, M. Giaccagli, B. Hunnekens, D. Astolfi, T. Oomen and N. van de Wouw, Repetitive control for Luré-type systems: Application to mechanical ventilation, *IEEE Transactions on Control Systems Technology*, vol.31, no.4, pp.1819-1829, 2023.

[6] M. Zhang, C. Lu, S. Tian, Y. Wang, M. Wu and M. Iwasaki, Improved disturbance rejection in repetitive-control systems: Phase-compensated equivalent-input-disturbance approach, *IEEE Transactions on Industrial Electronics*, vol.71, no.10, pp.12942-12951, 2024.

[7] K. Ohnishi, M. Shibata and T. Murakami, Motion control for advanced mechatronics, *IEEE/ASME Transactions on Mechatronics*, vol.1, no.1, pp.56-67, 1996.

[8] K.-S. Kim, K.-H. Rew and S. Kim, Disturbance observer for estimating higher order disturbances in time series expansion, *IEEE Transactions on Automatic Control*, vol.55, no.8, pp.1905-1911, 2010.

[9] J. Na, R. Grino, R. C. Castello, X. Ren and Q. Chen, Repetitive controller for time-delay systems based on disturbance observer, *IET Control Theory and Applications*, vol.4, no.11, pp.2391-2404, 2010.

[10] E. Sariyildiz, R. Oboe and K. Ohnishi, Disturbance observer-based robust control and its applications: 35th anniversary overview, *IEEE Transactions on Industrial Electronics*, vol.67, no.3, pp.2042-2053, 2020.

[11] K. Ohnishi, K. Ohnishi and K. Miyachi, Torque-speed regulation of DC motor based on load torque estimation, *Proc. of IEEJ IPEC-TOKYO*, vol.2, pp.1209-1216, 1983.

[12] S. Komada and K. Ohnishi, Force feedback control of robot manipulator by the acceleration tracing orientation method, *IEEE Transactions on Industrial Electronics*, vol.37, no.1, pp.6-12, 1990.

[13] W.-H. Chen, J. Yang, L. Guo and S. Li, Disturbance-observer-based control and related methods – An overview, *IEEE Transactions on Industrial Electronics*, vol.63, no.2, pp.1083-1095, 2016.

[14] H. Muramatsu and S. Katsura, An adaptive periodic disturbance observer for periodic disturbance suppression, *IEEE Transactions on Industrial Informatics*, vol.14, no.10, pp.4446-4456, 2018.

[15] U. Javaid, H. Dong, S. Ijaz, T. Alkarkhi and M. Haque, High-performance adaptive attitude control of spacecraft with sliding mode disturbance observer, *IEEE Access*, vol.10, pp.42004-42013, 2022.

[16] T. T. Phuong, K. Ohishi, C. Mitsantisuk, Y. Yokokura, K. Ohnishi, R. Oboe and A. Sabanovic, Disturbance observer and Kalman filter based motion control realization, *IEEJ Journal of Industry Applications*, vol.7, no.1, pp.1-14, 2018.

[17] M. Zheng, S. Zhou and M. Tomizuka, A design methodology for disturbance observer with application to precision motion control: An H-infinity based approach, *2017 American Control Conference*, pp.3524-3529, 2017.
[18] R. Sanchis Llopis, D. Tena Tena and I. Peñarrocha Alós, Cascade multi-resonant disturbance observer design: Application to a distillation column, *Journal of Process Control*, vol.132, Article no.103105, 2023.
[19] T. Mita, M. Hirata, K. Murata and H. Zhang, H_∞ control versus disturbance-observer-based control, *IEEE Transactions on Industrial Electronics*, vol.45, no.3, pp.488-495, 1998.
[20] H. Kobayashi, S. Katsura and K. Ohnishi, An analysis of parameter variations of disturbance observer for motion control, *IEEE Transactions on Industrial Electronics*, vol.54, no.6, pp.3413-3421, 2007.
[21] K. Yamada, I. Murakami, Y. Ando, T. Hagiwara, Y. Imai and M. Kobayashi, The parameterization of all disturbance observers, *ICIC Express Letters*, vol.2, no.4, pp.421-426, 2008.
[22] S. Phukapak, D. Koyama, K. Hashikura, M. A. S. Kamal and K. Yamada, The parameterizations of all disturbance observers for periodic output disturbances, *International Journal of Innovative Computing, Information and Control*, vol.19, no.1, pp.163-180, 2023.
[23] S. Phukapak, D. Koyama, K. Hashikura, M. A. S. Kamal, I. Murakami and K. Yamada, The parameterization of all disturbance observers for periodic input disturbances, *ECTI Transactions on Electrical Engineering, Electronics, and Communications*, vol.21, no.2, Article no.249809, 2023.
[24] S. Phukapak, D. Koyama, K. Hashikura, M. A. S. Kamal and K. Yamada, The parameterization of all disturbance observers for periodic input and output disturbances, *International Journal of Innovative Computing, Information and Control*, vol.19, no.3, pp.637-654, 2023.
[25] S. Phukapak, T. H. Do, D. Koyama, C. Phukapak, N. T. Mai, K. Hashikura, M. A. S. Kamal, I. Murakami and K. Yamada, Proposal of multi-period disturbance observers for periodic output disturbances, *ICIC Express Letters*, vol.18, no.7, pp.711-720, 2024.
[26] Y. Yamada, H. M. Tien, S. Phukapak, C. Phukapak, N. T. Mai, K. Hashikura, M. A. S. Kamal, I. Murakami and K. Yamada, Control system to attenuate periodic disturbance without using repetitive control, *International Journal of Innovative Computing, Information and Control*, vol.20, no.5, pp.1381-1397, 2024.
[27] M. Vidyasagar, *Control System Synthesis – A Factorization Approach*, MIT Press, 1985.
[28] B. A. Francis and W. M. Wonham, The internal model principle of control theory, *Automatica*, vol.12, no.5, pp.457-465, 1976.

Author Biography

Siripong Sangsarpan received the B.Eng. degree in Engineering from King Mongkut's Institute of Technology Ladkrabang (KMITL), Thailand, in 2012, and the M.Eng. degree from Thai-Nichi Institute of Technology (TNI), Thailand, in 2017. He is currently a doctoral student in the Graduate School of Science and Technology at Gunma University, Japan, and a lecturer at Thai-Nichi Institute of Technology, Thailand. His research interests include disturbance observers, robust control, and adaptive systems.

Daisuke Koyama received the B.S. degree in Science from Gunma University, Japan, 2017 and the M.S. degree in Science and Technology from Gunma University, Japan, 2020. Mr. Koyama is currently a doctoral candidate in Mechanical Science and Technology at Gunma University, Japan. His research interests include robust control system design.

Nghia Thi Mai received the B.S., M.S., and Dr. Eng. degrees from Gunma University, Japan, in 2009, 2011, and 2014, respectively. She is currently a lecturer at the Faculty of Electronics Engineering 1, Posts and Telecommunications Institute of Technology (PTIT), Vietnam, and a visiting associate professor at Gunma University, Japan. Her research interests include Smith predictor, internal model control, and robotics.

Md Abdus Samad Kamal received the B.Sc. degree in Electrical and Electronic Engineering from Khulna University of Engineering and Technology (KUET), Bangladesh, in 1997; and the M.S. and Dr. Eng. degrees from Kyushu University, Japan, in 2003 and 2006, respectively. He is currently an associate professor at the Graduate School of Science and Technology, Gunma University, Japan. His current research interests are reinforcement learning, intelligent transportation systems, and multiagent systems. He is a member of IEEE and SICE.

Iwanori Murakami received the B.E., M.E. and Dr. Eng. degrees from Gunma University, Japan, in 1992, 1994 and 1997, respectively. He is currently an associate professor at Gunma University, Japan. His research interests include robotics, applied electromagnetics, machines, and superconducting levitation applications.

Kou Yamada received B.S. and M.S. degrees from Yamagata University, Japan in 1987 and 1989, respectively, and a Dr. Eng. degree from Osaka University, Japan in 1997. From 1991 to 2000, he was with the Department of Electrical and Information Engineering, Yamagata University, Japan as a research associate. From 2000 to 2008, he was an associate professor in the Department of Mechanical System Engineering, Gunma University, Japan. Since 2008, he has been a professor in the Graduate School of Science and Technology, Gunma University, Japan. His research interests include robust control, repetitive control, process control, and control theory for inverse systems and infinite-dimensional systems. Dr. Yamada received the 2005 Yokoyama Award in Science and Technology, the 2005 Electrical Engineering/Electronics, Computer, Telecommunication, and Information Technology International Conference (ECTI-CON2005) Best Paper Award, the Japanese Ergonomics Society Encouragement Award for an Academic Paper in 2007, the 2008 Electrical Engineering/Electronics, Computer, Telecommunication, Information Technology International Conference (ECTI-CON2008) Best Paper Award, and the 4th International Conference on Innovative Computing, Information and Control Best Paper Award in 2009, the 14th International Conference on Innovative Computing, Information and Control Best Paper Award in 2019, and Outstanding Achievement Award from Kanto Branch of Japanese Society for Engineering Education in 2022 and JSME (The Japan Society of Mechanical Engineers) Education Award in 2023. He is a member of IEEE and SICE, and a fellow of JSME.